Hepatitis C Virus NS3 ATPase/Helicase: An ATP Switch Regulates the Cooperativity among the Different Substrate Binding Sites†

Giada Aurora Locatelli, Silvio Spadari, and Giovanni Maga*

Istituto di Genetica Molecolare, IGM-CNR, I-27100 Pavia, Italy

Received May 7, 2002; Revised Manuscript Received June 25, 2002

ABSTRACT: The protease/helicase NS3 is believed to play a central role in the replication cycle of the hepatitis C virus (HCV), and, therefore, it is an attractive target for antiviral chemotherapy. Several enzymological studies and crystallographic structures are available for the NS3 protease and helicase domains individually, but less is known about the NTPase and helicase activities of the full-length protein. The aim of our study was to characterize from an enzymological point of view the mechanism of interaction of the full-length NS3 protease/helicase with its nucleic acid (NA) and ATP substrates. Our kinetic analysis revealed that both the NA and ATP substrates can interact cooperatively with the enzyme through the coordinated action of two binding sites. Moreover, the observation of a reciprocal influence of both substrates on the kinetics of their interaction with the enzyme suggested that the NS3 helicase works as a dimer which can exist in three functionally different states: (i) an unbound state, with two equivalent low-affinity binding sites for ATP, which shows cooperative high-affinity NA binding; (ii) an ATP-bound state, with two equivalent low-affinity NA binding sites; and (iii) a NA-bound state, with two equivalent high-affinity ATP binding sites. The cycling between these different conformational states is thus regulated by an ATP switch. These results are discussed in light of the current models for NA unwinding by the HCV NS3 helicase.

Hepatitis C virus (HCV)[1] is a member of the Flaviviridae family of viruses and is responsible for most transfusion-associated cases of non-A, non-B hepatitis infecting more than 3% of the world population. HCV contains a positive single-stranded RNA genome of approximately 9.6 kb, encoding a polyprotein of about 3010 amino acids, that is processed by cellular and virus-encoded proteases. This proteolytic processing generates mature core (C), envelope (E), and nonstructural (NS) proteins. The protease/helicase NS3 protein and the RNA-dependent RNA polymerase NS5B protein are thought to be involved in the replication of the viral genome. These enzymes represent possible targets for more effective therapeutic agents, and we have focused our attention on the nonstructural protein 3 (NS3).

The HCV NS3 protein is a bifunctional enzyme exhibiting serine protease and RNA helicase activities which have been mapped to the N- and C-terminal domains, respectively (*1*). Numerous studies have demonstrated that the protease and helicase domains can be expressed independently and isolated as catalytically active species (*2*−*7*). Helicases catalyze the unwinding of dsDNA and RNA during cellular processes such as replication, recombination, transcription, splicing, and translation. In particular, the HCV helicase has unique properties since it is able to unwind also DNA/DNA homo- and RNA/DNA heteroduplexes in a 3′ to 5′ direction using several NTPs or dNTPs as the energy source (*8*, *9*). In a recent study, NS3 was shown to be a processive helicase on DNA substrates, whereas it required the NS4A cofactor to achieve optimal activity on RNA templates (*10*). In in vitro experiments the NS3 helicase requires a 3′ overhang region, which is proposed to provide an initiation site for unwinding duplex NA (*11*). The structure of the NS3 helicase domain consists of three subdomains that form a Y-shaped molecule: the NTPase subdomain containing an highly conserved bipartite NTP binding domain (Walker A and B motifs), the RNA binding subdomain that contains a conserved RNA binding motif, and a helical subdomain that contains no functionally conserved motifs. The NTPase and helicase active sites are linked with a shallow groove, but the RNA binding subdomain is distinctly separated by a deep interdomain cleft. The size of the interdomain cleft is adequate for binding ss DNA only (*12*, *13*).

Presently, it is not known whether NS3 is active as a monomer or as a multimer. The oligomerization of NS3 protein was investigated by protein−protein cross-linking (*14*), and it was shown that the helicase domain of HCV was capable of forming oligomers. In particular, in the absence of DNA, the cross-linked products were predominantly octamers, while in the presence of NA, protein dimers were the major accumulated species, even if in solution monomers of the protein were also present. A study of protein−protein interaction among all the HCV proteins with the yeast two-hybrid system gave another clue about the

† This work was supported by ISS-AIDS Grant 30C.70 (to S.S.) and by the CNR Target Project on Biotechnology (to S.S.). G.A.L. was the recipient of a Buzzati−Traverso Fellowship (420).

* Correspondence should be addressed to this author at the Istituto di Genetica Molecolare, IGM-CNR, via Abbiategrasso 207, I-27100 Pavia, Italy. Fax: 39 (0382)422286. E-mail: maga@igbe.pv.cnr.it.

[1] Abbreviations: HCV, hepatitis C virus; ss, single-stranded; ds, double-stranded; sp, singly primed; NTPs, ribonucleoside triphosphates; dNTPs, deoxynucleoside triphosphates; NA, nucleic acid; AU, absorbance unit(s); r(U), polyuridylic acid.

10.1021/bi026082g CCC: $22.00
Published on Web 07/20/2002

ability of NS3 to form dimers (*15*). In fact, the NS3 protein was shown to be able to self-interact. The minimal region for interaction was identified as the domain containing the NTP binding, NTPase, and helicase activities. The other domains of the protein were shown to be important for the stability of the dimer. Since the oligomerization has been proposed to enhance the helicase activity, helicase mutants defective in self-interaction were studied to verify whether they were able to unwind the NA or not. Three mutations were found that were able to perturb both the dimerization and the helicase activities. Since all three mutants interacted with the substrate, their reduction in helicase activity could be attributed to a reduction in dimer formation (*15*).

Based on the crystal structure of the RNA helicase domain, either alone or with a bound oligonucleotide, it was possible to propose two hypothetic models of unwinding of RNA and DNA duplexes (*12*, *13*). The process of unwinding requires helicases to translocate along the substrate in a unidirectional manner. During the translocation, the helicase has to bind and release the NA in a cyclical manner. In one model (*13*), the binding of ATP to the NS3 helicase was proposed to lead to a conformational change in the enzyme determining a closure of the cleft between the domain involved in the binding of the β-phosphate of ATP and the domain that interacts with the single-stranded polynucleotide. The hydrolysis of ATP would then result in opening of the cleft and release of ADP, possibly aiding protein translocation along the NA lattice of several bases. A second model was proposed, based on the construction of a molecular model of a dimeric NS3 helicase using the crystal structure of the monomeric enzyme (*12*). In such a model, the RNA binding motif of the two interacting monomers formed a channel in the middle of the dimer. The NA is positioned in the channel in such a way that one molecule of RNA helicase interacts with the ss RNA more extensively, whereas the other one makes less contacts with the bound NA. Thus, the two monomers, once interacting to form a dimer, were hypothesized to be not functionally equivalent. The ATP binding was proposed to result in a decrease of the affinity of HCV RNA helicase for the ss RNA, and ATP hydrolysis would cause the dissociation of the substrate from the enzyme. The ss RNA can then be bound by the other molecule of NS3 through rotation of the dimer. In this way, only one strand of the RNA can pass through the channel allowing the unwinding of the dsRNA.

All these models have been built on the structure of the helicase domain alone. Since the NS3 protein contains also a protease domain, we have determinated the enzymological parameters of the full-length protein, with the aim of investigatint its mechanism of interaction with the substrates of the reaction. Our data indicate that the NS3 helicase interacts with both the ATP and the NA substrates through a cooperative action of its binding sites, which is, in turn, regulated by an ATP switch.

MATERIALS AND METHODS

Preparation of Nucleic Acid Substrates. For the preparation of the 5′-end-labeled sp d24:d66-mer or d18:d66-mer DNA templates, the d24-mer or d18-mer primers were labeled with T4 polynucleotide kinase (Ambion) and [γ-^{32}P]ATP, according to the manufacturer's protocol. After removal of unincorporated ATP on a Sephadex G-25 column, the appropriate 5′-end-labeled primer was mixed at a 1:1 molar ratio with the d66-mer template in 20 mM Tris-HCl (pH 8.0) containing 20 mM KCl and 1 mM EDTA, heated at 65 °C for 5 min, and then slowly cooled at room temperature. The concentrations of the d66-mer, d18-mer, d36-mer, and d24-mer were calculated according to their molar extinction coefficients (758 760, 193 820, 383 470, and 250 950 M^{-1} cm^{-1}, respectively).

Sequences of the NA Used in This Study. d18-mer: 5′-GTTATGTACCTACTAAAC-3′. d24-mer: 5′-CTCGGAA-AATTTTTTGTTTTAGGT-3′. d36-mer: 5′-CTCGGAAAA-TTTTTTGTTTTAGGTCTGTATCAATAG-3′.d66-mer: 5′-AGGATGTAT**GTTTAGTAGGTACATAAC**TATCTAT-TGATACAGACCTAAAACAAAAAATTTTCCGAG-3′. The underlined and boldface sequences correspond to the regions complementary to the d24-mer and d18-mer, respectively. $r(U)_{18}$: 5′-UUUUUUUUUUUUUUUUUU-3′.

Protein Purification. Escherichia coli DH5α were cotransformed with the plasmid pAW3 (*16*) encoding the histidine-tagged NS3 protein. A 6 mL culture was grown overnight in LB broth (pH 7.5) at 37 °C. An aliquot of 4.5 mL of the overnight culture was used to inoculate a 90 mL culture in LB broth (pH 7.5) at 37 °C. The culture was grown to OD = 0.5 and then induced with IPTG (0.5 mM). The induction proceeded for 3 h at 25 °C; then the cells were harvested by centrifugation at 4000 rpm for 15 min in a Beckman JA20 rotor. Cell lysis was performed in Buffer A (50 mM NaH_2PO_4, pH 8.0, 300 mM NaCl, and 10 mM imidazole). The lysate was sonicated, and the suspension was centrifuged at 9000 rpm for 10 min in a Beckman JA20 rotor. NS3 in the supernatant was purified by chromatography through a FPLC-NiNTA column, which was first washed for 40 min with 10 mL of Buffer B (50 mM NaH_2PO_4, pH 8.0, 300 mM NaCl, 20 mM imidazole). NS3 protein bound to the column was eluted with Buffer B containing 250 mM imidazole. The fractions containing the homogeneous NS3 protein were identified by SDS−PAGE followed by Coomassie staining. The concentration of the HCV NS3 protein was determined spectrophotometrically using a molar extinction coefficient of 64 200 M^{-1} cm^{-1}.

Spectrophotometric Measurements. Absorbance was measured with an Ultrospec 2001*pro* spectrophotometer (Amersham Biosciencies) in a 300 μL quartz cuvette. A final volume of 300 μL contained 20−50 nM NS3 protein, 50 mM Tris-HCl (pH 7.5), 5 mM $MgCl_2$, and NA as indicated in the figure legends. Samples containing the NA substrate without enzyme were measured and subtracted as background. Binding reactions were started by addition of the enzyme. Samples were equilibrated at room temperature (25 °C) before measurement. Each measurement was repeated at least 3 times, and the mean values were used for the interpolation.

ATPase Activity Assays. The NTPase activity was determined by directly monitoring [γ-^{32}P]ATP hydrolysis by thin-layer chromatography. A final volume of 5 μL contained the following: 10 nM NS3 protein, 50 mM Tris-HCl (pH 7.5), 5 mM $MgCl_2$, 0.1 mM ATP, 50 μM $r(U)_{18}$, and 0.33 μM [γ-^{32}P]ATP, unless otherwise stated in the figure legends. Samples were incubated for 15 min at 25 °C and dotted onto sheets of PEI-cellulose. The products were separated by ascending chromatography with 0.5 M KH_2PO_4 (pH 3.4).

The intensities of the radioactive bands corresponding to ATP and P_i were quantified by densitometric scanning with a PhosphoImager.

Helicase Assays. The NS3 helicase activity assay was performed in a 15 μL reaction volume containing the following: 10 nM NS3 protein, 5 mM Tris-HCl (pH 7.5), 5 mM $MgCl_2$, 25 nM ^{32}P-labeled partial duplex DNA substrate, and 5 mM ATP, unless otherwise stated in the figure legends. The reaction was incubated for 20 min at 25 °C, and then stopped with 1 μL of termination buffer (10% glycerol, 0.0015% bromophenol blue, 0.0015% xylene cyanol FF, and 10 mM EDTA). Aliquots were analyzed on a native 8% polyacrylamide gel. The intensities of the radioactive bands corresponding to ds18:66-mer and ss18-mer were quantified by densitometric scanning with a PhosphoImager.

Bandshift Assay. For the bandshift assays, the ^{32}P-labeled partial duplexes d24:d66-mer and d18:d66-mer were used. The final volume of the reactions was 15 μL containing 50 nM NS3 helicase protein, 5 mM Tris-HCl (pH 7.5), 5 mM $MgCl_2$, 5 mM ATP, and ^{32}P-labeled partial duplex DNA substrate as indicated in the figure legends. The reaction was incubated for 20 min at 25 °C and stopped with 1 μL of termination buffer (10% glycerol, 0.0015% bromophenol blue, 0.0015% xylene cyanol FF, and 10mM EDTA). Aliquots were analyzed on a native 8% polyacrylamide gel. The intensities of the radioactive bands corresponding to NA alone and complexed with the NS3 protein were quantified by densitometric scanning with a PhosphoImager.

Calculation of Kinetic Parameters. For determination of reaction velocities, the products formed in the ATPase and helicase reactions were measured at different time intervals, in the presence of increasing concentrations of the reaction substrates. The slopes of the linear plots of the measured values versus time, representing the initial velocities of the reaction, were replotted as the dependence on substrate concentrations. At least six different time points were used for each substrate concentration. The K_m and V_{max} values were calculated by non-least-squares computer fitting of the experimental data to the appropriate rate equations, derived from the kinetic scheme reported in Figure 6C.

For analysis of the absorbance−quenching experiments, the fractional absorbance at 220 nm (FAU_{220}) was defined as the ratio between the AU_{220} value measured in the presence of NA and the corresponding value measured in its absence. The dependence of FAU_{220} on the NA concentrations was fitted to the equation:

$$1 - FAU_{220} = (FAU_{max}[NA]^n)/(K_D + [NA]^n) \quad (1)$$

where FAU_{max} is the fractional absorbance corresponding to maximal quenching of the protein, K_D is the equilibrium dissociation constant, and n is the cooperativity parameter.

The time dependence of FAU_{220} at a fixed NA concentration was fitted to a simple exponential equation in the form:

$$FAU_{220} = A(e^{-k_{obs}t}) \quad (2)$$

where A is the burst amplitude, t is time, and k_{obs} is the relaxation rate. The k_1 and k_{-1} rate values for NA binding and dissociation were calculated from the k_{obs} values according to the equations:

$$k_{obs} = k_1([NA] + K_D) \quad (3)$$

and

$$k_{obs} = k_1[NA] + k_{-1} \quad (4)$$

The dependence of the burst amplitude A on NA concentration was fitted to the equation:

$$1 - A = (A_{max}[NA]^n)/(K_D + [NA]^n) \quad (5)$$

The time-dependent dissociation of NA from NS3 was fitted to either a simple exponential or a double exponential in the form:

$$A_1(e^{-k't}) + A_2(e^{-kt}) \quad (6)$$

where k' and k are the rates for the fast and slow dissociation phases, respectively.

RESULTS

Cooperative Binding of HCV NS3 Helicase to a Nucleic Acid Substrate in the Absence of ATP. To assess the binding kinetics of a NA substrate to the NS3 protein, the decrease in the intrinsic absorbance of the protein upon NA binding was monitored spectrophotometrically. The absorbance of NS3 was measured spectrophotometrically by continuous scanning in the 200−300 nm wavelength interval after 180 s of incubation upon addition of increasing amounts of a DNA oligonucleotide. The DNA/DNA oligonucleotide d24:d66-mer was used as the NA substrate. This substrate has a 42-nt ss tail at its 5′-template end, but no ss DNA tail at its 3′-template end; thus, it is not a substrate for the helicase activity of NS3, even if it still binds to the enzyme (*9*). At the very low concentrations used in the binding assays (20−50 nM), the absorbance at 280 nm (tryptophan and tyrosine residues) of the recombinant full-length NS3 protein used in this study was negligible (<0.01 AU), whereas significant absorbance (≈0.1−0.2 AU) was observed at 220 nm (peptidic bonds). The DNA oligonucleotide, on the other hand, absorbed maximally at 260 nm. As shown in Figure 1A, the absorbance (corrected for the background given by the added DNA) decreased in a DNA concentration-dependent manner. The residual absorbance was related to the enzyme−substrate complex formed as described under Materials and Methods. Fitting of the values of the residual absorbance as a dependence of the DNA concentration (Figure 1B) was consistent with a cooperative mode of binding [K_D = 225 (±10) nM, n = 1.7 (±0.2)]. As shown in Figure 1C, absorbance−quenching time course experiments with increasing concentrations of this oligonucleotide showed simple exponential kinetics. The enzyme−substrate formation reached the equilibrium after 180 s, with a plateau of the FAU_{220} corresponding to the quenching of 70% of the total absorbance (data not shown). Fitting of the burst amplitude (which was proportional to the amount of E−NA complex formed) to the DNA concentration showed again a cooperative mode of binding with a K_D value of 290 (±5) nM and an n value of 1.8 (±0.1) (Figure 1D). The k_1 and k_{-1} values for the d24:d66-mer substrate (according to the kinetic scheme shown in Figure 6C) were calculated from the k_{obs} values as described and are summarized in Table 1.

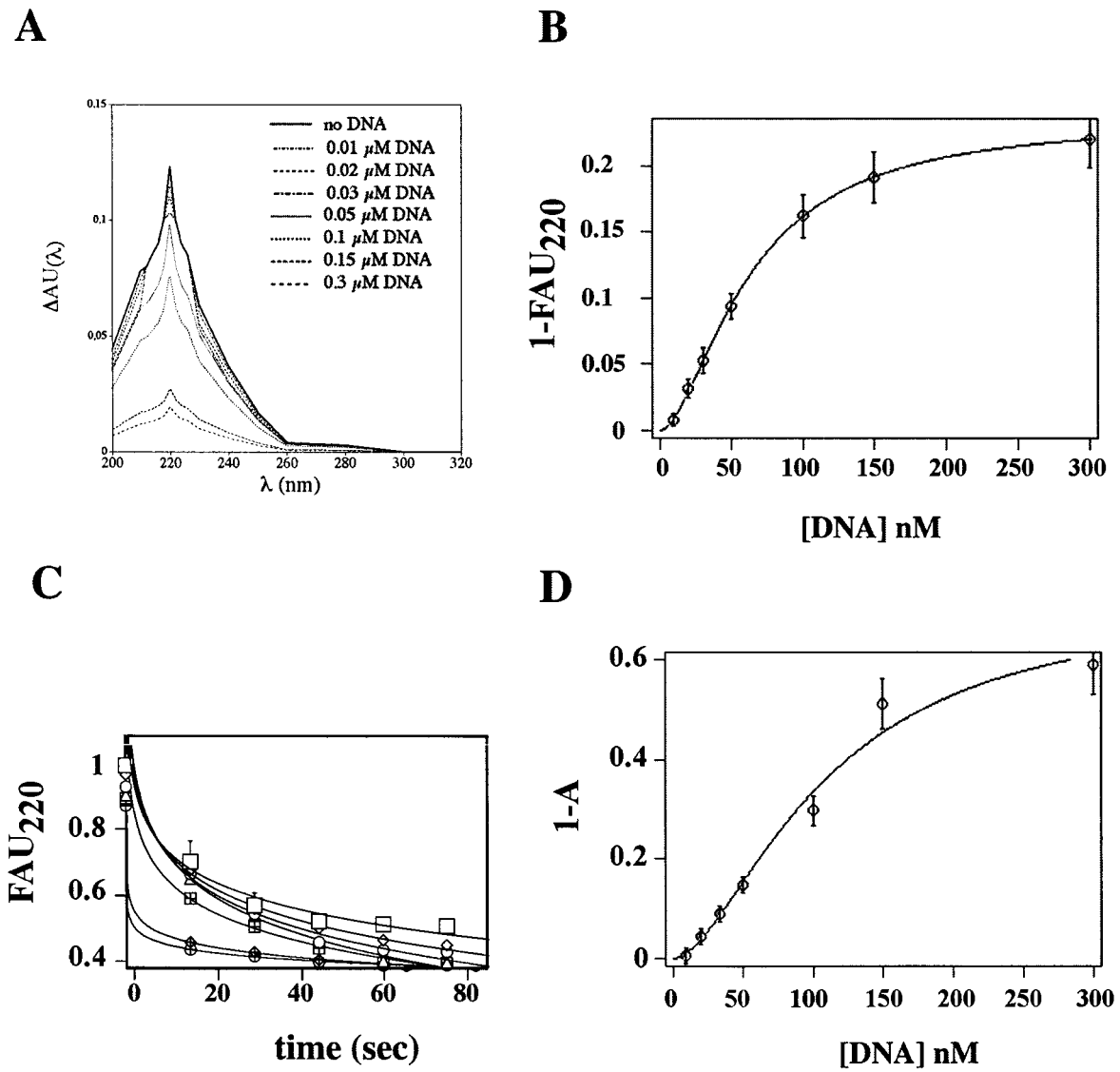

FIGURE 1: Cooperative binding of HCV NS3 helicase to a nucleic acid substrate in the absence of ATP. (A) UV−absorbance profile of HCV NS3 in the absence or in the presence of increasing amounts of d24:d66-mer. Measurements were performed as described under Materials and Methods. Only the absorbance of NS3 is shown, corrected for the background given by the DNA. DNA concentrations used were 10 (squares), 20 (rhombics), 30 (circles), 50 (triangles), 100 (crossed squares), 150 (crossed rhombics), and 300 (crossed circles) nM, respectively. (B) Dependence of the fractional absorbance FAU_{220} on the d24:d66-mer concentration. Data were fitted to eq 1 (see Materials and Methods) by the nonlinear least-squares curve-fitting method. Error bars represent ±SD for the mean values of three independent measurements. (C) Time course of NS3 absorbance quenching by d24:d66-mer. Fixed concentrations of DNA were incubated in the presence of 10 nM enzyme, and absorbance was monitored until the reaction reached equilibrium (180 s). Data are shown for the first 80 s and were fitted to eq 2 by the nonlinear least-squares curve-fitting method. Error bars represent ±SD for the mean values of three independent measurements. DNA concentrations tested were 10, 20, 30, 50, 100, 150, and 300 nM. Measured rates (k_{obs}) were 0.12 (±0.02), 0.17 (±0.05), 0.22 (±0.05), and 0.38 (±0.07) s^{-1}, respectively. These values were used to calculate k_1 and k_{-1} values as described under Materials and Methods. The k_1 and k_{-1} estimates are listed in Table 1. (D) Dependence of the burst amplitude on the d24:d66-mer concentration. Burst amplitudes from the experiments shown in panel C were fitted to eq 5 by the nonlinear least-squares curve-fitting method. Error bars represent ±SD for the mean values of three independent measurements.

Binding of NS3 Helicase to a Short Single-Stranded RNA Oligonucleotide Is Not Cooperative. Previous kinetic studies have suggested that the average binding site for NS3 on a ss RNA or DNA has the size of about 5−10 nt. These observations have been confirmed directly by the crystallographic resolution of the structure of the NS3 helicase bound to a ss oligonucleotide, which showed that the binding site of the NS3 helicase domain covered six residues of ss dU oligonucleotide. To study the kinetics of interaction of the full-length NS3 protein with a short ss RNA, a time course absorbance−quenching experiment was performed with a ss $r(U)_{18}$ oligonucleotide. As shown in Figure 2A, addition of $r(U)_{18}$ to the reaction mixture in the presence of increasing amounts of NS3 protein revealed simple exponential kinetics. When similar experiments were performed in the presence of increasing $r(U)_{18}$ concentrations, similar kinetics were observed (Figure 2B). The concentration dependence of the burst amplitude was fitted to an hyperbolic equation as shown in Figure 2C to give a K_D value of 0.87 (±0.1) μM and a cooperativity index (n) of 1.1 (±0.2). From the k_{obs} values, the binding and dissociation rates k_1 and k_{-1} (according to the kinetic scheme shown in Figure 6C) were calculated and are summarized in Table 1. A possible explanation for the lack of cooperativity for binding of the $r(U)_{18}$ with respect to the d24:d66 oligonucleotide might be that NS3 binds as a monomer to the RNA oligonucleotide

Table 1: Kinetic Parameters for Nucleic Acid Binding to HCV NS3

	−ATP						+ATP		
substrate	K_D (μM)	K'_D (μM)	k_1 ($\mu M^{-1} s^{-1}$)	k_{-1} (s^{-1})	k'_{-1} (s^{-1})	n	K_D (μM)	k_{-1} (s^{-1})	n
d24:d66	0.22[a]					1.7[a]	0.64[f]	0.16[f]	
	0.21[b]		0.25[b]	0.05[b]		1.8[b]			
	0.27[c]					1.8[c]			
	0.2[d]	0.67[d]		0.035[d]	0.25[d]				
d18:d66	0.18					1.7	0.44[g]		1.1
ss d18-mer	0.75					1.2			
ss d24-mer	0.4					1.5			
ss d36-mer	0.25		0.24[e]	0.06[e]		1.7			
ss d66-mer	0.22					1.9			
ss $r(U)_{18}$	0.87		0.23	0.19		1.1	1.2[g]		0.87

[a] From the experiment shown in Figure 1B; ±SD values are indicated in the text. [b] From the experiment shown in Figure 1D; ±SD values are indicated in the text. [c] From the experiment shown in Figure 4A; ±SD values are indicated in the text. [d] From the bandshift experiment shown in Figure 4C. K_D, K'_D and k_{-1}, k'_{-1} refer to the affinity vlaues and dissociation rates for high- and low-affinity binding modes, respectively. ±SD values are indicated in the text. [e] From the experiment shown in Figure 3C; ±SD values are indicated in the text. [f] From the experiment shown in Figure 4C; the k_{-1} value in the presence of ATP was calculated and used for the estimation of the K_D value assuming a k_1 of 0.25 $\mu M^{-1} s^{-1}$. ±SD values are indicated in the text. [g] The K_D values derived from the experiments shown in Figure 5B and 5D are indeed K_m values, and should be considered an upper estimate of the true K_D. ±SD values are indicated in the text.

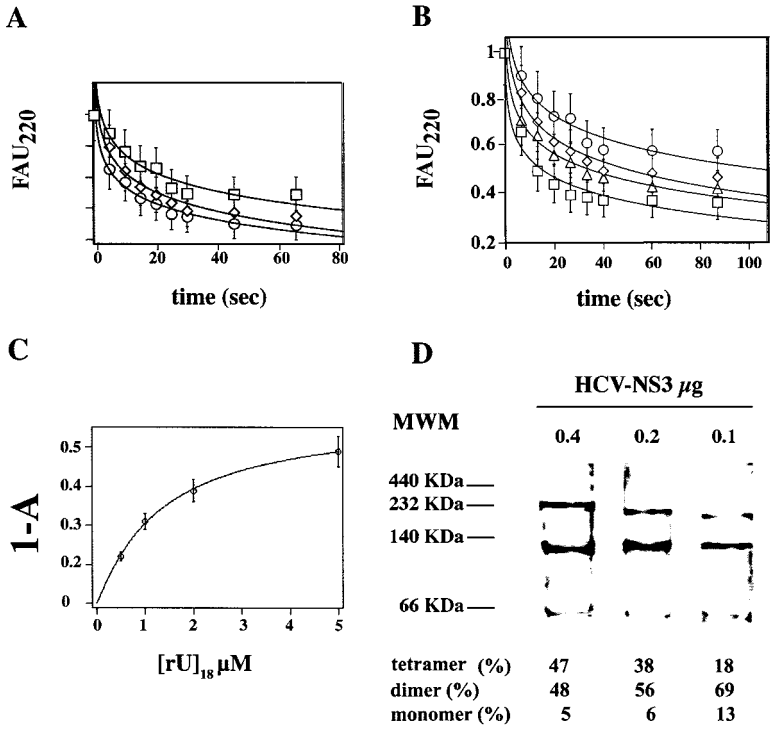

FIGURE 2: Binding of NS3 helicase to a short single-stranded RNA oligonucleotide is not cooperative. (A) Time course of NS3 absorbance quenching by ss $r(U)_{18}$. Increasing concentrations of NS3 were incubated in the presence of 500 nM $r(U)_{18}$, and absorbance was monitored until the reaction reached equilibrium (180 s). Data are shown for the first 80 s and were fitted to eq 2 by the nonlinear least-squares curve-fitting method. Error bars represent ±SD for the mean values of three independent measurements. NS3 concentrations tested were 75 (squares), 100 (triangles), and 150 nM (circles). (B) Time course of NS3 absorbance quenching by ss $r(U)_{18}$. Fixed concentrations of $r(U)_{18}$ were incubated in the presence of 100 nM enzyme, and absorbance was monitored until the reaction reached equilibrium (180 s). Data are shown for the first 90 s of the reaction and were fitted to eq 2 by the nonlinear least-squares curve-fitting method. Error bars represent ±SD for the mean values of three independent measurements. RNA concentrations tested were 0.5 (circles), 1(rhombics), 2 (triangles), and 5 μM (squares). Measured rates (k_{obs}) were 0.16 (±0.12), 0.22 (±0.15), 0.37 (±0.05), and 0.65 (±0.07) s^{-1}, respectively. These values were used to calculate k_1 and k_{-1} values as described under Materials and Methods. The k_1 and k_{-1} estimates are listed in Table 1. (C) Dependence of the burst amplitude on the $r(U)_{18}$ concentration. Burst amplitudes from the experiments shown in panel B were fitted to eq 5 by the nonlinear least-squares curve-fitting method. Error bars represent ±SD for the mean values of three independent measurements. (D) Native-PAGE analysis of NS3. Increasing amounts of protein were incubated in the presence of 50 μM $r(U)_{18}$ for 10 min at 25 °C and subjected to 5% glutaraldehyde fixation for an additonal 5 min, before analysis on a 8% native polyacrylamide gel. Proteins were revealed by silver staining. The intensities of the bands were measured by scanning densitometry, corrected for the background (empty lane), and used to calculate the relative percentages of the different forms (monomer, dimer, and tetramer) at each NS3 concentration, which are indicated at the bottom of the respective lanes.

and as a dimer to the DNA substrate. However, it has been reported that the presence of a ss RNA oligonucleotide is necessary and sufficient to promote dimerization of HCV NS3. To assess the oligomeric state of our protein, we performed glutaraldehyde cross-linking in the presence of $r(U)_{18}$, followed by native gel electrophoresis. As shown in

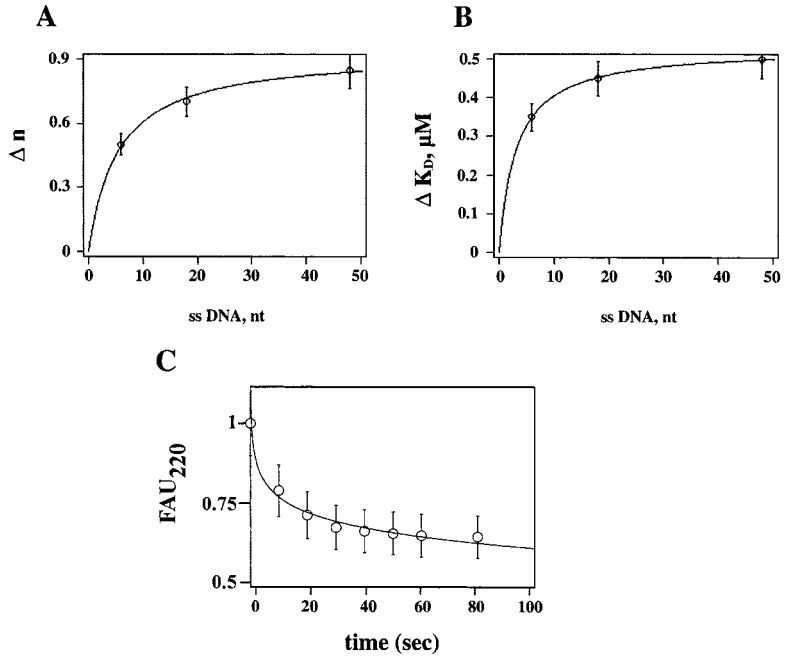

FIGURE 3: Affinity and cooperativity of HCV NS3 binding to ss DNA are dependent on the lattice length. Binding kinetics of NS3 to ss DNA oligonucleotides of 18, 24, 36, and 66 nt were measured spectrophotometrically as described under Materials and Methods, and the corresponding calculated n and K_D values are listed in Table 1. (A) Dependence of the cooperativity index (n) on the length of the DNA lattice. The increase in the n values, Δn, defined as the difference between the n values calculated for the 24, 36, and 66 nt oligonucleotides and the value for the 18 nt oligonucleotide, was plotted as a dependence of the increasing DNA lattice length. Tha value of 18 nt was taken as the starting point, and the differences from 18 to 24, 36, and 66 were reported on the x-axis. Data were fitted to the hyperbolic equation: $\Delta n = \Delta n_{max}/(1 + [nt_{0.5}]/[nt])$, where Δn_{max} is the maximal increase in cooperativity and $[nt_{0.5}]$ is the increase in ss DNA length required to give half of the maximal increase in cooperativity. (B) Dependence of the affinity (K_D) on the length of the DNA lattice. The decrease in the K_D values, ΔK_D, defined as the difference between the K_D value calculated for the 18 nt oligonucleotide and the corresponding values for the 24, 36, and 66 nt oligonucleotides, was plotted as a dependence of the increasing DNA lattice length. Tha value of 18 nt was taken as the starting point, and the differences from 18 to 24, 36, and 66 nt were reported on the x-axis. Data were fitted to the hyperbolic equation: $\Delta K_D = \Delta_{max}/(1 + [nt_{0.5}]/[nt])$, where Δ_{max} is the maximal decrease in the K_D value and $[nt_{0.5}]$ is the increase in ss DNA length required to give half of the maximal increase in affinity. (C) Time course of NS3 absorbance quenching by ss 36-mer DNA oligonucleotide. 1 μM ss 36-mer was incubated in the presence of 100 nM enzyme and absorbance monitored until the reaction reached equilibrium (180 s). Data are shown for the first 80 s of the reaction. Data were fitted to eq 2 by the nonlinear least-squares curve-fitting method. Error bars represent ±SD for the mean values of three independent measurements. The burst rate (k_{obs}) was 0.35 (±0.1) s^{-1}. This value was used to calculate k_1 and k_{-1} values as described under Materials and Methods.

Figure 2D, the major cross-linked products were dimers, with a shift toward the tetrameric form at high protein concentration, indicating that the NS3 protein multimerized in the presence of $r(U)_{18}$. The apparent decrease in the electrophoretic mobility of the band corresponding to the tetramers observed at increasing protein concentrations was an artifact probably due to a change in the shape/mass ratio, an effect often experienced during electrophoresis of high molecular weight protein complexes under nondenaturing conditions. Together, these results suggested that the difference in binding kinetics between the d24:d66-mer and the $r(U)_{18}$ oligonucleotides was likely due to a different number of occupied binding sites within the multimeric NS3 protein.

The Affinity and Cooperativity of HCV NS3 Binding to ss DNA Are Dependent on the Lattice Length. The results summarized above suggested that a cooperative binding of NS3 to a NA substrate might occur only when the ss region available for binding can accommodate both monomers. To directly test this hypothesis, the kinetics of NS3 binding to ss DNA oligonucleotides of increasing lengths were studied spectrophotometrically, using the same experimental approach utilized for studying the binding to the d24:d66-mer DNA (Figure 1). As summarized in Table 1, increasing lengths of the ss DNA lattice (18, 24, 36, and 66 nt) led to an increase in affinity with K_D values of 0.75 (±0.1), 0.4 (±0.05), 0.25 (±0.03), and 0.22 (±0.02) μM, respectively. A parallel increase in the cooperativity index was observed, with n values of 1.2 (±0.1), 1.5 (±0.2), 1.7 (±0.2), and 1.9 (±0.2), respectively. Interestingly, the K_D and n values for the ss 18-mer DNA oligonucleotide were comparable to the ones measured for the ss $r(U)_{18}$ RNA, suggesting that the major determinant of binding affinity was the length of the NA lattice and not its RNA or DNA nature. The increase both in the cooperativity index (Δn) and in the affinity (ΔK_D) as a dependence of the ss DNA length was fitted to a hyperbolic equation. As shown in Figure 3A,B, the ss DNA length required for the transition from a noncooperative to a cooperative mode of binding was estimated as 22 (±1) nt. A maximal n value of 1.96 (±0.02) and a maximal affinity of 200 (±10) nM were also calculated. Figure 3C shows the time-dependent association of HCV NS3 to the 36-mer ss DNA oligonucleotide. The curve showed simple exponential kinetics, and from the observed rate a k_1 value of 0.33 (±0.03) μM^{-1} s^{-1} and a k_{-1} value of 0.09 (±0.01) s^{-1} were calculated. These values are in good agreement with the corresponding ones estimated for HCV NS3 binding to the d24/d66-mer DNA oligonucleotide, which bears a 42-nt-long ss strand. These results reinforced the hypothesis that the major determinant for substrate binding was the ss part of the NA substrate.

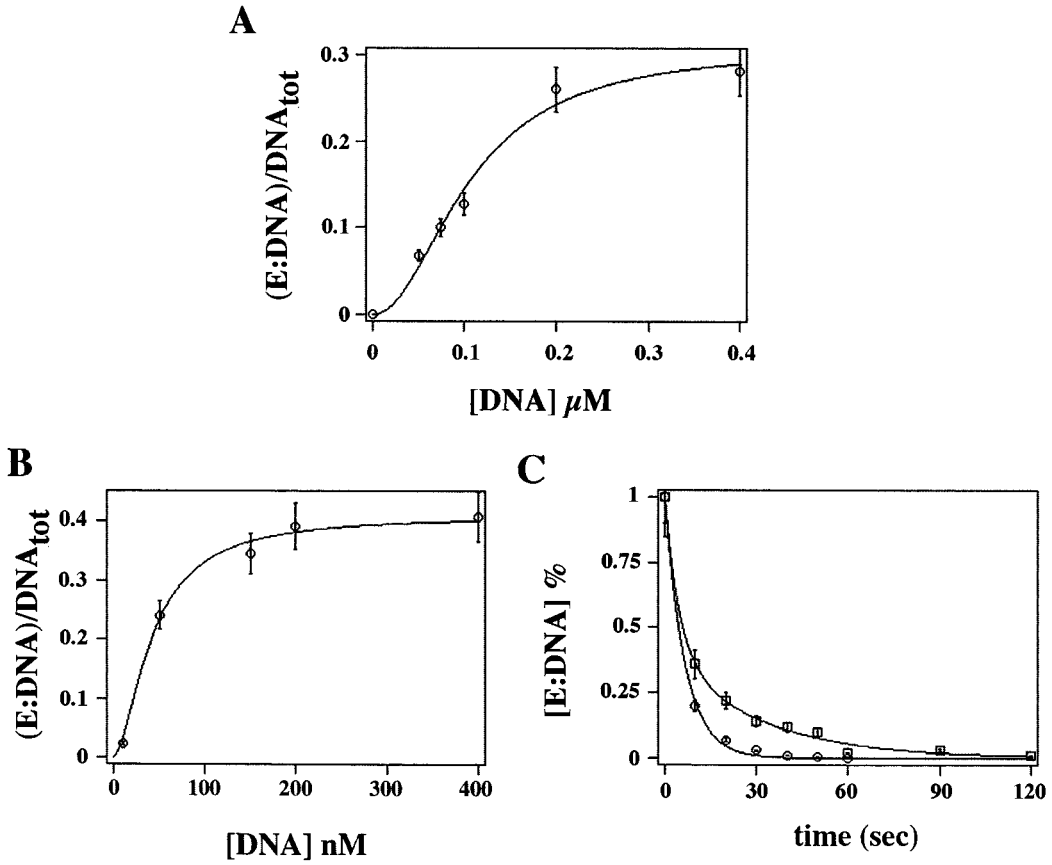

FIGURE 4: Dissociation of the d24:d66-mer DNA substrate from HCV NS3 is biphasic. (A) Bandshift experiments with NS3 and increasing concentrations of d24:d66-mer substrate (indicated on the *x*-axis) were performed as described under Materials and Methods. The normalized amount of enzyme−DNA complex formed in the experiment was plotted as a dependence of the input DNA concentration. Data were fitted to the equation: [Bound/Bound+Free] = [Bound/Bound+Free]$_{max}$/(K_D + [DNA]^n), where [Bound/Bound+Free]$_{max}$ represents the maximum relative amount of DNA shifted and *n* is the cooperativity index. Data were fitted by the nonlinear least-squares curve-fitting method. Error bars represent ±SD for the mean values of three independent measurements. (B) Bandshift experiments with NS3 and increasing concentrations of d18:d66-mer substrate were performed as described under Materials and Methods. The normalized amount of enzyme−DNA complex formed was plotted as a dependence of the input DNA concentration. Data were fitted to the equation: [Bound/Bound+Free] = [Bound/Bound+Free]$_{max}$/(K_D + [DNA]^n), where [Bound/Bound+Free]$_{max}$ represents the maximum relative amount of DNA shifted and *n* is the cooperativity index. Data were fitted by the nonlinear least-squares curve-fitting method. Error bars represent ±SD for the mean values of three independent measurements. (C) Dissociation of NS3 from a DNA template. 50 nM NS3 was incubated 10 min at 25 °C in the presence of 250 nM d24:d66-mer and in the absence (circles) or in the presence (squares) of 5 mM ATP. Samples were then taken at the indicated time intervals and fixed with 5% glutaraldehyde before analysis on a 8% native polyacrylamide gel. The relative amount of enzyme−substrate complex, defined as [E:DNA]$_t$/[E:DNA]$_0$, was plotted versus time. Data were fitted either to a simple exponential (squares) or to eq 6 (circles) by the nonlinear least-squares curve-fitting method. Error bars represent ±SD for the mean values of three independent measurements.

Dissociation of the d24:d66-mer DNA Substrate from HCV NS3 Is Biphasic. To confirm the spectrophotometric measurements, the equilibrium binding and dissociation kinetics for the d24:d66-mer substrate were investigated through gel-retardation assays with radiolabeled DNA substrate. Incubation of a fixed concentration of NS3 with increasing amounts of labeled d24:d66-mer DNA template showed a concentration-dependent formation of the enzyme−substrate complex. Binding kinetics were found to be cooperative (Figure 4A) with a K_D value of 269 (±20) nM and an *n* value of 1.8 (±0.2). Binding experiments in the absence of ATP were performed also with a d18:d66-mer oligonucleotide, with a 39 nt ss DNA tail at its 3′-template end. This has been shown to be a good substrate for the NS3 helicase activity (*9*). As in the case of the d24:d66-mer, cooperative kinetics of binding were observed (Figure 4B) with a K_D value of 180 (±15) nM and an *n* of 1.7 (±0.1). To directly determine the dissociation rate of the enzyme from the DNA template, fixed amounts of NS3 protein and labeled d24:d66-mer were incubated for 3 min in order to reach the equilibrium, and then samples were withdrawn at different time points and subjected to glutaraldehyde fixation before native gel electrophoresis analysis. As shown in Figure 4C, a time-dependent decrease of the shifted enzyme−substrate complex was observed. The best fit of the experimental data was obtained with a double-exponential model, indicative of a biphasic mode of dissociation. The corresponding k'_{-1}, k_{-1} values were estimated to be 0.25 (±0.05) s^{-1} and 0.035 (±0.003) s^{-1}, respectively. Using a k_1 value of 0.25 μM^{-1} s^{-1}, two affinity values (K'_D, K_D) could be calculated and were 1 (±0.4) μM and 0.14 (±0.03) μM, respectively (Table 1). Taken together, these data indicated that NS3 possesses two nonequivalent NA binding sites which interacted cooperatively with the d24:d66-mer DNA.

The Cooperative Binding of a Nucleic Acid Substrate to NS3 Is Modulated by ATP Hydrolysis. Next, dissociation of NS3 from the d24:d66-mer DNA substrate was measured in the presence of 5 mM ATP. As shown in Figure 4C, the

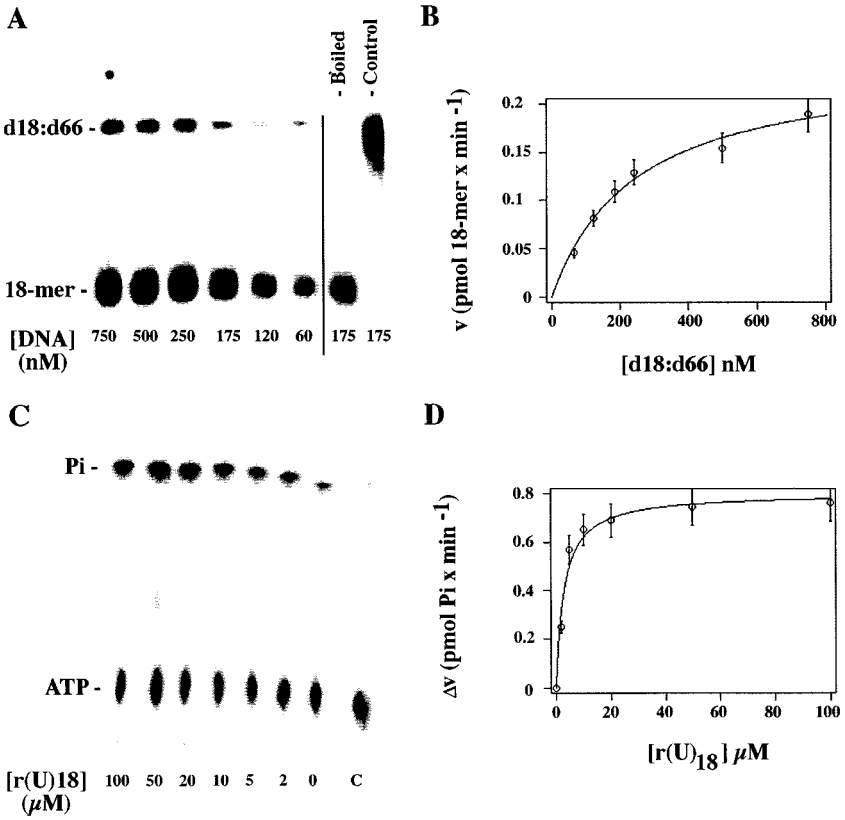

FIGURE 5: Cooperative binding of a nucleic acid substrate to NS3 is modulated by ATP hydrolysis. (A) The helicase assay with increasing concentrations of the d18:d66-mer substrate (indicated on bottom of the gel) was performed as described under Materials and Methods. Boiled: control with 175 nM template heated 5 min at 95 °C before loading. Control: reaction with 175 nM substrate without enzyme. (B) Dependence of the helicase reaction velocity on the substrate concentration. Initial velocity values for the helicase reaction were determined as described under Materials and Methods and plotted versus substrate concentrations. Error bars represent ±SD for the mean values of three independent measurements. (C) ATPase assay in the presence of increasing amounts of $r(U)_{18}$ (indicated on bottom of the PEI-TLC) was performed as described under Materials and Methods. C: control lane without NS3 enzyme. (D) Dependence of the increase in ATPase reaction velocity (Δv), defined as $v_{(rU)} - v_o$, on the $r(U)_{18}$ concentration. Initial velocity values for the ATPase reaction were determined as described under Materials and Methods and plotted versus the substrate concentrations. Error bars represent ±SD for the mean values of three independent measurements.

dissociation was monophasic, following a simple exponential, and the calculated dissociation rate of 0.16 (±0.02) s^{-1} was comparable to the one observed for the rapid phase measured in the absence of ATP, k'_{-1} (Table 1). The corresponding K_D value was 0.64 μM. It was not possible to measure the binding of NS3 to the d18:d66-mer oligonucleotide in the presence of ATP by gel-retardation assay, due to the helicase activity, which caused fast release of the 18-mer product and enzyme dissociation. Also, using a nonhydrolyzable analogue of ATP was not advisable, since it has been already shown that the dissociation rate of NS3 from a DNA template is influenced by the nature of the nucleotide triphosphate (*9*). However, titration of the DNA substrate in a helicase assay (Figure 5A) allowed the determination of the DNA concentration dependence of the strand displacement activity. As shown in Figure 5B, no cooperativity ($n = 1.1 \pm 0.1$) was observed for DNA binding under these conditions, with a K_m value of 240 (±20) nM and a steady-state rate (k_{cat}) value of 0.45 (±0.02) s^{-1}, very close to the dissociation rate value determined for the d24:d66-mer DNA template in the presence of ATP (Table 1).

It has been shown that homopolymeric RNAs can stimulate the ATPase activity of the NS3 protein. Thus, increasing amounts of $r(U)_{18}$ were titrated into an ATPase assay (Figure 5C), and the kinetics of binding of $r(U)_{18}$ to the enzyme were studied by measuring the increase in the ATPase catalytic rate as a dependence of the $r(U)_{18}$ concentration. Similarly to the experiments with the enzyme alone, in the presence of ATP, $r(U)_{18}$ association showed no cooperativity, with an n value of 0.87 (±0.07) and a K_m value of 1.2 (±0.2) μM, as shown in Figure 5D. The k_{cat} for ATP hydrolysis was 1.33 (±0.06) s^{-1}. It should be mentioned that the K_m values derived with this approach are only upper-limit estimates of the true K_D values. However, these experiments indicated that inclusion of ATP abolished the cooperativity of NA binding.

ATP Hydrolysis by the NS3 Enzyme Is Modulated by Nucleic Acid Binding. The experiments described above suggested a modulatory effect of ATP binding on the kinetics of association of the NS3 enzyme to a NA substrate. Next, the effects of the absence or presence of NA on ATP hydrolysis were studied. The results are summarized in Table 2. When increasing amounts of ATP were titrated into an ATPase reaction in the absence of NA, no cooperativity of binding was observed with an n value of 0.83 (±0.03) and a K_m of 1.5 (±0.07) mM (Figure 6A). Parallel experiments were performed in the presence of a fixed amount of $r(U)_{18}$. Under these conditions, clear cooperativity for ATP binding was observed, with an n value of 1.8 (±0.05) and a K_m of 0.47 (±0.05) mM (Figure 6A). The k_{cat} for ATP hydrolysis was 1.75 (±0.05) s^{-1}. On the other hand, when the dependence of the helicase reaction on the ATP concentration

Table 2: Kinetic Parameters for ATP Binding and Hydrolysis by the HCV NS3 Protein

	no NA[a]	+r(U)$_{18}$[a]	+d18:d66-mer[b]
K_D		0.47 (±0.05) mM	0.5 (±0.06) mM
K'_D	1.5 (±0.07) mM		
n	0.83 (±0.03)	1.8 (±0.05)	1.1 (±0.1)
k_{cat}	1.75 (±0.05)[a] s^{-1}	1.75 (±0.05)[a] s^{-1}	0.49 (±0.05)[b] s^{-1}

[a] ATPase assay. The k_{cat} value is the maximal rate of ATP hydrolysis. [b] Helicase assay. The k_{cat} value is the maximal rate of 18-mer displacement.

was studied, no cooperativity was observed, with an n value of 1.1 (±0.1), a K_m of 0.5 (±0.06) mM, and a k_{cat} of 0.49 (±0.05) s^{-1} (Figure 6B).

DISCUSSION

Increasing evidence suggests that the NS3 protease/helicase of HCV functions as an oligomer, most likely a dimer, in an analogous manner to other DNA and RNA helicases (*14*, *15*). Enzymological and structural studies led to the proposal of a model for NA unwinding by NS3 (*12*, *13*). These studies, however, refer to the helicase domain alone, whereas less is known on the enzymological properties of the full-length NS3 protein, comprising both the helicase and the protease domain (*8*, *10*, *16*, *17*). We have performed a detailed kinetic analysis of the interaction of the full-length NS3 with its substrates ATP and NA. Our analysis suggests that the NS3 helicase can exists in three different functional states: (i) a substrate-unbound state, with two equivalent low-affinity binding sites for ATP which shows cooperative high-affinity NA binding; (ii) an ATP-bound state, with two equivalent low-affinity NA binding sites; and (iii) a NA-bound state, with two equivalent high-affinity ATP binding sites. When only one monomer was bound to NA [as in the case of the ss 18-mer DNA or the ss r(U)$_{18}$ RNA], an intermediate state was observed, with two nonequivalent ATP binding sites. In fact, in the absence of ATP, with a NA substrate bearing a long ss region, cooperative kinetics have been observed for binding to the enzyme, consistent with the involvement of two sites. On the other hand, with a short ss oligonucleotide, not long enough to accommodate two NS3 molecules, binding was noncooperative. From these binding studies, the second-order association constant k_1, according to the kinetic scheme in Figure 6C, has been determined for both substrates. We found that HCV NS3 bound the ss r(U)$_{18}$ RNA substrate with the same rate with respect to either a ss 36-mer or a d24/d66-mer DNA oligonucleotide (k_1 values were 0.23 μM^{-1} s^{-1} for the RNA and 0.24 or 0.25 μM^{-1} s^{-1} for the two DNA templates, respectively), but its dissociation from the ss RNA template was faster than from both DNA substrates (k_{-1} values were 0.19 s^{-1} for RNA and 0.06 or 0.05 s^{-1} for the DNA templates, respectively). With the d24/d66-mer DNA substrate, we observed biphasic dissociation kinetics with two different rates (k_{-1} and k'_{-1}, according to the kinetic scheme in Figure 6C). The fast rate of dissociation (k'_{-1}) is equivalent to the rate of dissociation of the ss r(U)$_{18}$ oligonucleotide, whereas the slow rate (k_{-1}) is consistent with the estimated dissociation rate for the ss 36-mer oligonucleotide. It is interesting to note that by using the k_1 value calculated by direct binding experiments, two different K_D values could be estimated for the sites, with the larger one (corresponding to the low-affinity site) almost identical to the K_D value observed for both the ss RNA r(U)$_{18}$ and the ss DNA 18-mer oligonucleotides (Table 1). In addition, we found that the affinity and cooperativity of HCV NS3 binding to DNA were dependent on the length of the ss lattice. From the increase of the cooperativity and of the affinity values as a dependence of the ss DNA length (Figure 3A,B), a maximal n value of 1.96 (±0.02) and a maximal affinity of 200 (±10) nM have been estimated. From these data, the ss DNA length required to induce the transition from a noncooperative to a cooperative mode of binding has been estimated as 22 (±1) nt. Previous pre-steady-state kinetic studies have shown that the nature (i.e., RNA vs DNA composition) of short ss oligonucleotides did not influence the K_D values for NS3 binding, whereas a significant increase in affinity was shown for both r(U)$_n$ and d(U)$_n$ oligonucleotides as their length increased from 5 to 25 nt (*18*). Our data are in agreement with these observations. Protein−protein cross-linking and native gel analysis showed that NS3 is in a predominantly dimeric form also when bound to the short RNA r(U)$_{18}$ (Figure 2D). The monomer:dimer:tetramer molar ratios are 1:5.3:1.3 at 0.1 μg of protein, 1:9.3:6.3 at 0.2 μg of protein, and 1:9.6:9.4 at 0.4 μg of protein, suggesting that the dimeric form is the most thermodynamically favored, reaching equilibrium between 0.2 and 0.4 μg of NS3, whereas the tetramers are formed at higher protein concentrations. Altogether, these results suggest that only one monomer is bound to either the ss r(U)$_{18}$ or the ss 18-mer, or, alternatively, that two molecules of NA can independently bind to the two monomers with identical affinity. On the other hand, when a longer ss NA region is available, binding of the first monomer to the NA substrate facilitates subsequent binding of the second monomer, leading to cooperative kinetics. It has been proposed by structural studies that binding of a NA to a dimeric NS3 can stabilize the enzyme−substrate complex (*12*). The kinetic data presented here further support this hypothesis. ATP was found to regulate the cooperative association of NS3 to the NA. In fact, in the presence of ATP, no cooperativity was observed for binding of NA to the enzyme. Direct dissociation studies in the presence of ATP revealed a simple exponential time-dependence with a rate equal to the one measured for the dissociation from the low-affinity binding site in the absence of ATP (k'_{-1}) (Figure 4D). The corresponding K_D value was also consistent with the values observed for binding of the short (18 nt) NA substrates (Table 1). Thus, the presence of ATP induced a transition in the dimeric NS3 from a high-affinity to a low-affinity state for NA binding. This effect of ATP has been already proposed by others as well as by our group (*8*, *9*). When ATP binding was analyzed, it became clear that the NA substrate could also influence the interaction of NS3 with ATP. In the absence of NA, simple binding kinetics for ATP were observed in an ATPase assay, with a K_m of 1.5 mM. However, when the short r(U)$_{18}$ oligonucleotide was added, cooperative binding was observed, with a K_m of 0.45 mM (Figure 6A). These data indicate that the NS3 dimer in the absence of NA is composed of two equivalent low-affinity binding sites for ATP. When, however, one of the two sites is bound to NA, the two monomers become not equivalent anymore, and one of the two sites is converted into a high-affinity state for ATP. We could not determine whether NA binding increased the affinity for ATP of the bound monomer

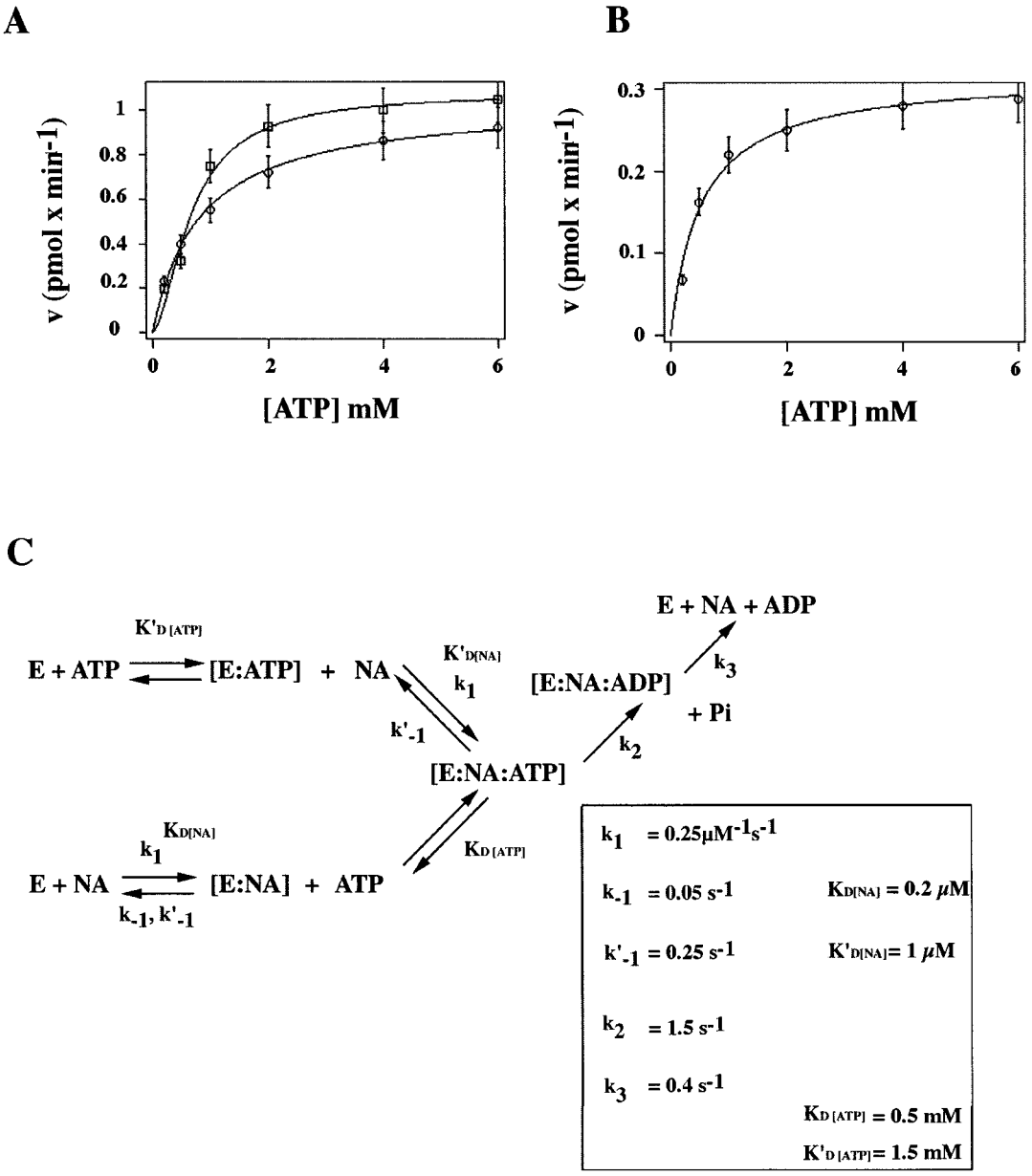

FIGURE 6: ATP hydrolysis by the NS3 enzyme is modulated by nucleic acid binding. (A) Dependence of the ATPase reaction velocity in the absence (circles) or in the presence (squares) of $r(U)_{18}$ on the ATP concentration. Initial velocity values for the ATPase reaction were determined as described under Materials and Methods and plotted versus substrate concentrations. Error bars represent ±SD for the mean values of three independent measurements. (B) Dependence of the helicase reaction velocity on the ATP concentration. Initial velocity values for the helicase reaction were determined as described under Materials and Methods and plotted versus the substrate concentrations. Error bars represent ±SD for the mean values of three independent measurements. (C) Schematic reaction pathway for the NS3 NTPase/helicase reaction. According to the model proposed in the text, the NS3 enzyme is shown to bind NA in the absence of ATP (lower branch) with a high-affinity constant ($K_{D[NA]}$) through the cooperative interaction of two sites with two different dissociation rates, k_{-1} and k'_{-1}. Subsequent binding of ATP to the E:NA complex is shown to be governed by the high-affinity constant $K_{D[ATP]}$. Conversely, NS3 binds ATP in the absence of NA (upper branch) with the low-affinity constant $K'_{D[ATP]}$. Subsequent binding of NA to the E:ATP complex is shown to occur through the low-affinity constant $K_{D[NA]}$ characterized by the fast dissociation rate k'_{-1}. The NA association rate k_1 is equal for both branches of the reaction. The value of k_2 was taken as the catalytic rate of ATP hydrolysis, whereas the value of k_3 was set equal to the rate of strand displacement. For details, see text.

or, alternatively, induced a global conformational change which made the NA-unbound monomer bind ATP with higher affinity. Notably, when ATP was titrated in a helicase assay with a NA substrate bearing a longer ss region, no cooperativity was observed, and the K_m value for ATP was close to the K_D value measured for the high-affinity state (Figure 6B). This observation is consistent with our hypothesis that when both monomers are bound to NA, both ATP sites are converted into the high-affinity state. From the kinetic constants derived in this work, we could estimate a requirement of 1 molecule of ATP every 4−6 displaced nucleotides. This is a lower limit, since the strand displacement reaction at equilibrium was very likely limited by the dissociation rate of the enzyme from the NA substrate, as suggested by the very similar values of k_{cat} and k'_{-1} (Figure 6C). Models for the action of the NS3 helicase (*12, 13*) propose a cycling between different conformational states of the protein. We provide evidence that the cycling between different functional states (corresponding to high- and low-affinity NA binding modes) could be regulated by an ATP

switch, as already hypothesized from structural studies. In addition, our data show that ATP binding is enhanced by binding of NA to the enzyme.

In conclusion, our results add further support to the hypothesis that HCV NS3 NTPase/helicase works as a dimer. The estimated values for the kinetic constants for the different steps of the reaction are summarized in Figure 6C. We have indicated as K_D and K'_D the equilibrium dissociation constants for the high- and low-affinity states, respectively. We were not able to determine the association and dissociation rates for ATP; thus, they are not indicated in the reaction pathway, and the steps involving ATP binding are described by equilibrium constants only. The catalytic rate of ATP hydrolysis has been assigned to k_2, whereas the rate k_3 has been considered equal to the measured catalytic rate for strand displacement. Since our data have been obtained with a full-length protein, comprising also the protease domain, it would be of interest to investigate whether a cooperative mode of interaction with the substrates occurs also for the protease domain. During the revision process of this paper, a work has been published by Levin and Patel where the authors, using fluorometric techniques, analyzed the DNA binding properties of the helicase domain of the HCV NS3 protein (*19*). They observed a minimal ss DNA binding site of 8 nt and also binding of multiple NS3 molecules with ss DNAs longer than 15 nt. These results are in good agreement with the ones presented in our study. Interestingly, these authors failed to detect cooperative binding of NS3 to DNA. Since only the helicase domain has been used, their data, together with our data obtained with the full-length protein, suggest that the protease domain might be responsible for the observed multimerization of HCV NS3.

Given the current limitations of available in vivo or ex vivo methodologies to study the HCV infection, biochemical studies still play a major role in investigating the HCV biology and in the identification of metabolic pathways susceptible to inhibition.

ACKNOWLEDGMENT

We thank Dr. M. J. McGarvey, Department of Medicine, Imperial College School of Medicine, London, for kindly providing us with the expression vector pAW3 encoding the full-length HCV NS3 protein.

REFERENCES

1. Kwong, A. D., Kim, J. L., and Lin, C. (2000) *Curr. Top. Microbiol. Immunol. 242*, 171−196.
2. Suzich, J. A., Tamura, J. K., Palmer-Hill, F., Warrener, P., Grakoui, A., Rice, C. M., Feinstone, S. M., and Collett, M. S. (1993) *J. Virol. 67* (10), 6152−6158.
3. Jin, L., and Peterson, D. L. (1995) *Arch. Biochem. Biophys. 323* (1), 47−53.
4. Tai, C. L., Chi, W. K., Chen, D. S., and Hwang, L. H. (1996) *J. Virol. 70* (12), 8477−8484.
5. Landro, J. A., Raybuck, S. A., Luong, Y. P., O'Malley, E. T., Harbeson, S. L., Morgenstern, K. A., Rao, G., and Livingston, D. J. (1997) *Biochemistry 36* (31), 9340−9348.
6. Kwong, A. D., Kim, J. L., Rao, G., Lipovsek, D., and Raybuck, S. A. (1999) *Antiviral Res. 41* (1), 67−84.
7. Lin, C., and Kim, J. L. (1999) *J. Virol. 73* (10), 8798−8807.
8. Paolini, C., De Francesco, R., and Gallinari, P. (2000) *J. Gen. Virol. 81* (Pt. 5), 1335−1345.
9. Locatelli, G. A., Gosselin, G., Spadari, S., and Maga, G. (2001) *J. Mol. Biol. 313* (4), 683−694.
10. Pang, P. S., Jankowsky, E., Planet, P. J., and Pyle, A. M. (2002) *EMBO J. 21*, 1168−1176.
11. Tackett, A. J., Wei, L., Cameron, C. E., and Raney, K. D. (2001) *Nucleic Acids Res. 29* (2), 565−572.
12. Yao, N., Hesson, T., Cable, M., Hong, Z., Kwong, A. D., Le, H. V., and Weber, P. C. (1997) *Nat. Struct. Biol. 4* (6), 463−467.
13. Kim, J. L., Morgenstern, K. A., Griffith, J. P., Dwyer, M. D., Thomson, J. A., Murcko, M. A., Lin, C., and Caron, P. R. (1998) *Structure 6* (1), 89−100.
14. Levin, M. K., and Patel, S. S. (1999) *J. Biol. Chem. 274* (45), 31839−31846.
15. Khu, Y. L., Koh, E., Lim, S. P., Tan, Y. H., Brenner, S., Lim, S. G., Hong, W. J., and Goh, P. Y. (2001) *J. Virol. 75* (1), 205−214.
16. Wardell, A. D., Errington, W., Ciaramella, G., Merson, J., and McGarvey, M. J. (1999) *J. Gen. Virol. 80* (Pt. 3), 701−709.
17. Paolini, C., Lahm, A., De Francesco, R., and Gallinari, P. (2000) *J. Gen. Virol. 81* (Pt. 7), 1649−1658.
18. Preugschat, F., Averett, D. R., Clarke, B. E., and Porter, D. J. (1996) *J. Biol. Chem. 271* (40), 24449−24457.
19. Levin, M. K., and Patel, S. (2002) *J. Biol. Chem.* (in press).

BI026082G